Available online at www.sciencedirect.com
ScienceDirect
Polyhedron 26 (2007) 3577–3584
POLYHEDRON
www.elsevier.com/locate/poly

Synthesis, electrochemistry, MO properties, and X-ray diffraction structures of the new redox-active diphosphine ligand 2-(2-thienylidene)-4,5-bis(diphenylphosphino)-4-cyclopenten-1,3-dione (tbpcd) and the rhenium compound *fac*-BrRe$(CO)_3$(tbpcd)

William H. Watson [a,*], David Wiedenfeld [b,*], Aparna Pingali [c],
Bhaskar Poola [c], Michael G. Richmond [c,*]

[a] *Department of Chemistry, Texas Christian University, Fort Worth, TX 76129, United States*
[b] *Department of Chemistry, Marshall University, Huntington, WV 25755, United States*
[c] *Department of Chemistry, University of North Texas, Denton, TX 76203, United States*

Received 9 November 2006; accepted 25 March 2007
Available online 14 April 2007

Abstract

Knoevenagel condensation of 4,5-bis(diphenylphosphino)-4-cyclopenten-1,3-dione (bpcd) with thiophene-2-carboxaldehyde furnishes the second-generation unsaturated diphosphine ligand 2-(2-thienylidene)-4,5-bis(diphenylphosphino)-4-cyclopenten-1,3-dione (**1**, tbpcd) in high yield. The substitution chemistry of the rhenium compounds $BrRe(CO)_5$ and $BrRe(CO)_3(THF)_2$ with tbpcd has been investigated and found to produce *fac*-BrRe$(CO)_3$(tbpcd) (**2**). Compounds **1** and **2** have been isolated and fully characterized in solution by IR and NMR (^1H and ^{31}P) spectroscopies, in addition to mass spectrometry, and X-ray crystallography. The redox properties of **1** and **2** have been examined by cyclic voltammetry, and these data are discussed relative to the results obtained from extended Hückel MO calculations and emission spectroscopic studies, as well as related ligand derivatives previously prepared by us. Our data indicate that the lowest excited state in tbpcd and *fac*-BrRe$(CO)_3$(tbpcd) arises from a $\pi \rightarrow \pi^*$ intraligand (IL) transition confined exclusively to the tbpcd ligand.

Keywords: Diphosphine ligand; Electrochemistry; MO calculations; Photophysics; Rhenium complex

---

1. Introduction

Over the course of the last several decades, numerous rhenium(I) compounds based on $XRe(CO)_3(\alpha\text{-diimine})$ have been synthesized and examined as luminescent sensing devices [1], scaffolds for the construction of redox-active molecular switches and wires [2], and excited-state oxidants for the study of proton-coupled electron transfer processes [3]. One commonality between the different compounds described in these studies is the presence of a relatively low-lying π^* acceptor orbital associated with the α-diimine ligand that participates in metal-to-ligand charge transfer ($d\pi \rightarrow \pi^*$) upon optical excitation. Knowledge of the lifetime and the exact nature of the lowest emitting state(s) is crucial if the controlled manipulation of energy transfer and/or electron transfer manifolds are to be achieved.

Our groups have had an interest in the synthesis and photophysical study of new systems based on $XRe(CO)_3(\alpha\text{-diimine})$ but where the ancillary α-diimine ligand has been replaced by a bidentate ligand possessing different electron-reservoir properties. To this end, we have prepared new rhenium(I) compounds containing the redox-active ligands 2,3-bis(diphenylphosphino)maleic anhydride

---

[*] Corresponding authors. Tel.: +1 817 257 7195 (W.H. Watson), +1 304 696 2307 (D. Wiedenfeld), +1 940 565 3548 (M.G. Richmond).
E-mail addresses: w.watson@tcu.edu (W.H. Watson), wiedenfeld@marshall.edu (D. Wiedenfeld), cobalt@unt.edu (M.G. Richmond).

0277-5387/$ - see front matter © 2007 Elsevier Ltd. All rights reserved.
doi:10.1016/j.poly.2007.03.039

(bma) [4], 4,5-bis(diphenylphosphino)-4-cyclopenten-1,3-dione (bpcd) [5], and 2,3-bis(methylthio)pyrrolo[1,2-a]benzimidazol-1-one (bmpb) [6], the structures of which are shown below.

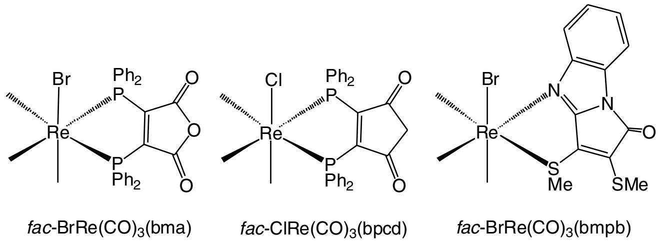

In terms of the diphosphine ligand bpcd, we recently confirmed that facile and significant structural modifications of the central dione platform could easily be achieved through Knoevenagel condensation reactions. Two such reactions involving the union of 9-anthracenecarboxaldehdye and ferrocenecarboxaldehyde are depicted in Scheme 1 [7,8]. The resulting second-generation ligands derived from bpcd can be custom- or fine-tuned to produce compounds that have a fixed or specific redox potential(s) by simply controlling the extent of π-electron delocalization within the diphosphine ligand platform. With the attachment of suitable donor–acceptor groups to the original dione scaffold, new ligands with the ability to function as directed energy transfer agents can be expected.

Wishing to extend our functionalization studies of the bcpd ligand to other aldehydes that could, in principle, function as multidentate ligand systems, we have studied the condensation reaction between thiophene-2-carboxaldehyde and bpcd. Herein we present our data on the synthesis of the new diphosphine ligand 2-(2-thienylidene)-4,5-bis(diphenylphosphino)-4-cyclopenten-1,3-dione (tbpcd). The reactivity of this ligand with $BrRe(CO)_5$ and $BrRe(CO)_3(THF)_2$ has been examined and found to give *fac*-$BrRe(CO)_3$(tbpcd) in high yield. Both new compounds have isolated and their solid-state structures determined. The redox properties and photophysics of the tbpcd ligand and its rhenium(I) complex have been investigated and the results are discussed relative to MO calculations at the extended Hückel level.

2. Experimental

2.1. General

The starting diphosphine ligand bpcd was prepared from 4,5-dichloro-4-cyclopenten-1,3-dione and Ph_2PSiMe_3 [9], while $BrRe(CO)_3(THF)_2$ was synthesized from $BrRe(CO)_5$ [10]. The thiophene-2-carboxaldehyde was purchased from Aldrich Chemical Co. and used as received. All reaction and NMR solvents were distilled from an appropriate drying agent using Schlenk techniques and stored under argon in storage vessels equipped with high-vacuum Teflon stopcocks [11]. The tetra-*n*-butylammonium perchlorate (TBAP) electrolyte was purchased from Johnson Matthey Electronics and was recrystallized from ethyl acetate/hexane, followed by drying under high vacuum for at least 36 h.

The IR spectral data were recorded on a Nicolet 20 SXB FT-IR spectrometer in sealed 0.1 mm NaCl cells, while the

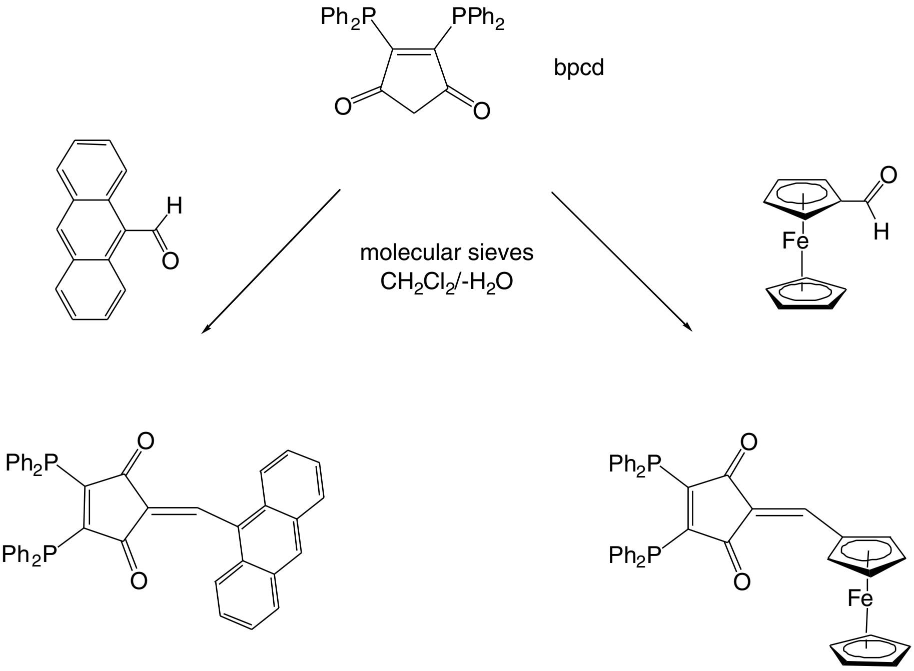

Scheme 1.

^{1}H spectral data were recorded at 200 MHz on a Varian Gemini-200 spectrometer. The ^{31}P NMR spectra were collected in the proton-decoupled mode on a Varian 300-VXR spectrometer at 121 MHz, with the reported chemical shifts referenced to external H_3PO_4 (85%), taken to have $\delta = 0$. The absorption spectra were recorded on a HP 8453 ChemStation (Marshall) or a HP 8425A diode array spectrometer (UNT). The emission data were recorded on a Jobin Fluorolog FL 3-22 spectrometer equipped with DataMax software. The ESI-APCI mass spectra were recorded at the University of the Pacific in the positive ionization mode for **1** and the negative ionization mode for **2**.

2.2. Synthesis of tbpcd (1)

To a small Schlenk vessel was added 0.20 g (0.43 mmol) of bpcd, followed by 25 mL of CH_2Cl_2, 0.39 mL (excess) thiophene-2-carboxaldehyde, and ca. 4.0 g of molecular sieves (4 Å). Stirring over night under argon led to the complete consumption of the bpcd ligand, as assessed by TLC analysis. The presence of the desired product was confirmed by TLC examination of the reaction solution. Here the tbpcd ligand was observed as an orange spot having a $R_f = 0.30$ using CH_2Cl_2/petroleum ether (3:2) as the eluent. The molecular sieves were filtered away and the solution concentrated to ca. 0.5 mL, after which the crude product was subjected to chromatographic separation over silica gel using the aforementioned solvent system to give tbpcd as an orange solid in 90% yield (0.22 g). IR (CH_2Cl_2): ν(CO) 1719 (m, symm dione), 1673 (vs, antisymm dione) cm^{-1}. ^{1}H NMR ($CDCl_3$): δ 7.05 (dd, 1H, thiophene, $^3J_{H–H} = 7$, 5 Hz), 7.22–7.46 (m, 20H, phenyls), 7.56 (s, 1H, vinyl), 7.68 (d, 1H, thiophene, $^3J_{H–H} = 7$ Hz), 7.90 (d, 1H, thiophene, $^3J_{H–H} = 5$ Hz). ^{31}P NMR ($CDCl_3$): δ −24.23 (AB quartet, $J_{P-P} = 25$ Hz). ESI-APCI MS (*m/z*): 581.086 [**1**+Na]$^+$, 558.995 [**1**]$^+$.

2.3. Synthesis of fac-BrRe(CO)$_3$(tbpcd) (2) from tbpcd and BrRe(CO)$_3$(THF)$_2$

To a Schlenk tube under argon was charged 0.10 g (0.20 mmol) of $BrRe(CO)_3(THF)_2$ and 0.11 g (0.20 mmol) of **1**, after which 20 mL of CH_2Cl_2 was added via cannula. The contents were stirred at room temperature for 3 h and examined by TLC, which revealed the complete consumption of the starting materials and only the presence of the desired product as a yellow spot at $R_f = 0.20$ using CH_2Cl_2 as the mobile phase. The solvent was concentrated and compound **2** subsequently isolated by column chromatography over silica gel using CH_2Cl_2. Yield of **2**: 0.14 g (80%). IR (CH_2Cl_2): ν(CO) 2039 (s), 1966 (s), 1912 (s), 1728 (vw, symm dione), 1684 (s, antisymm dione) cm^{-1}. ^{1}H NMR ($CDCl_3$): δ 7.21 (dd, 1H, thiophene, $^3J_{H–H} = 7$, 5 Hz), 7.32–7.90 [m, 22H, vinyl (1H), thiophene (1H), and phenyls (20H)], 8.06 (d, 1H, thiophene, $^3J_{H–H} = 5$ Hz). ^{31}P NMR ($CDCl_3$): δ 18.09 (s, 1P), 19.18 (s, 1P). ESI-APCI MS (*m/z*): 907.821 [**2**]$^-$, 938.922 [**2**+MeO]$^-$.

2.4. X-ray diffraction structures

Single crystals of the tbpcd ligand were grown from a CH_2Cl_2 solution containing tbpcd that had been layered with hexane, while X-ray quality crystals of *fac*-BrRe(CO)$_3$(tbpcd) were grown from an acetone solution containing *fac*-BrRe(CO)$_3$(tbpcd) that was layered with Et_2O. The reported X-ray data for both compounds were collected on a Bruker SMART™ 1000 CCD-based diffractometer at 213 K. The frames were integrated with the available SAINT software package using a narrow-frame algorithm [12], and the structures were solved and refined using the SHELXTL program package [13]. The molecular structures were checked by using PLATON [14], and solved by direct methods with all nonhydrogen atoms refined anisotropically. All carbon-bound hydrogen atoms were assigned calculated positions and allowed to ride on the attached heavy atom, unless otherwise noted. Refinement for tbpcd converged at $R = 0.0641$ and $R_w = 0.1187$ for 6379 independent reflections with $I > 2\sigma(I)$, with **2** · acetone yielding convergence values of at $R = 0.0358$ and $R_w = 0.0873$ for 8558 independent reflections with $I > 2\sigma(I)$. Tables 1 and 2 summarize the pertinent X-ray data for compounds **1** and **2** · acetone.

2.5. Electrochemistry

The cyclic voltammetric data were recorded on a PAR Model 273 potentiostat/galvanostat, equipped with positive feedback circuitry to compensate for *i*R drop. The

Table 1
X-ray crystallographic data and processing parameters for the ligand tbpcd (**1**) and *fac*-BrRe(CO)$_3$(tbpcd) · acetone (**2** · acetone)

Compound	**1**	**2** · acetone
CCDC entry no.	623341	623342
Crystal system	monoclinic	monoclinic
Space group	$P2_1/c$	$P2_1/c$
a (Å)	13.049(2)	15.986(3)
b (Å)	10.878(2)	15.761(3)
c (Å)	19.582(2)	14.522(3)
β (°)	93.461(3)	95.267(3)
V (Å^3)	2774.5(7)	3643(1)
Molecular formula	$C_{34}H_{24}O_2P_2S$	$C_{37}H_{24}BrO_5P_2ReS$ · acetone
Formula weight	558.53	966.75
Formula units per cell (*Z*)	4	4
D_{calc} (Mg/m^3)	1.337	1.763
λ (Mo Kα) (Å)	0.71073	0.71073
μ (mm^{-1})	0.263	4.625
R_{merge}	0.0550	0.0783
Absorption correction	empirical	empirical
Absorption correction factor	0.8149/0.6572	1.0000/0.4525
Total reflections	21 540	38 899
Independent reflections	6379	8558
Data/restraints/parameters	6379/0/353	8558/0/462
R	0.0641	0.0358
R_w	0.1187	0.0873
Goodness-of-fit on F^2	1.005	0.993
$\Delta\rho_{maximum}$, $\Delta\rho_{minimum}$ (e/Å^3)	0.490 and −0.261	1.978 and −1.290

Table 2
Selected bond distances (Å) and angles (°) in ligand tbpcd (**1**) and *fac*-$BrRe(CO)_3(tbpcd) \cdot$ acetone (**2** · acetone)

tbpcd (1)			
Bond distances			
S(1)–C(34)	1.693(3)	S(1)–C(31)	1.727(3)
C(1)–C(30)	1.352(3)	C(1)–C(5)	1.466(4)
C(1)–C(2)	1.473(3)	C(2)–C(3)	1.514(4)
C(3)–C(4)	1.355(3)	C(4)–C(5)	1.526(3)
C(30)–C(31)	1.436(3)	C(31)–C(32)	1.411(4)
C(32)–C(33)	1.398(4)	C(33)–C(34)	1.351(4)
P(1)· · ·P(2)	3.330(1)	S(1)· · ·O(2)	2.861(2)
Bond angles			
C(34)–S(1)–C(31)	91.5(1)	C(30)–C(1)–C(5)	131.1(2)
C(30)–C(1)–C(2)	121.9(2)	C(5)–C(1)–C(2)	107.0(2)
C(4)–C(3)–P(2)	121.7(2)	C(2)–C(3)–P(2)	128.4(2)
C(3)–C(4)–P(1)	122.9(2)	C(5)–C(4)–P(1)	128.2(2)
C(1)–C(30)–C(31)	132.8(2)	C(30)–C(31)–S(1)	127.6(2)
fac-BrRe(CO)$_4$(tbpcd) · acetone (2 · acetone)			
Bond distances			
Re(1)–P(2)	2.449(1)	Re(1)–P(1)	2.468(1)
Re(1)–Br(1)	2.6530(6)	S(1)–C(37)	1.676(5)
S(1)–C(34)	1.714(5)	C(1)–C(2)	1.342(5)
C(1)–C(5)	1.526(5)	C(2)–C(3)	1.513(6)
C(3)–C(4)	1.473(6)	C(4)–C(33)	1.365(6)
C(4)–C(5)	1.469(6)	C(33)–C(34)	1.430(6)
C(34)–C(35)	1.467(6)	C(35)–C(36)	1.355(7)
C(36)–C(37)	1.361(8)	P(1)· · ·P(2)	3.213(2)
S(1)· · ·O(2)	2.912(3)		
Bond angles			
C(32)–Re(1)–C(31)	91.0(2)	C(32)–Re(1)–C(30)	88.1(2)
C(31)–Re(1)–C(30)	90.1(2)	C(32)–Re(1)–P(2)	95.6(1)
C(31)–Re(1)–P(2)	92.5(1)	C(30)–Re(1)–P(2)	175.4(1)
C(32)–Re(1)–P(1)	95.4(1)	C(31)–Re(1)–P(1)	171.7(1)
C(30)–Re(1)–P(1)	95.4(1)	P(2)–Re(1)–P(1)	81.59(3)
C(32)–Re(1)–Br(1)	178.3(1)	C(31)–Re(1)–Br(1)	89.5(1)
C(30)–Re(1)–Br(1)	93.5(1)	P(2)–Re(1)–Br(1)	82.69(3)
P(1)–Re(1)–Br(1)	83.95(3)	C(37)–S(1)–C(34)	91.7(3)
C(2)–C(1)–P(1)	120.2(3)	C(5)–C(1)–P(1)	130.5(3)
C(1)–C(2)–P(2)	121.2(3)	C(3)–C(2)–P(2)	126.6(3)
C(5)–C(4)–C(3)	107.9(3)		

homemade three-electrode cell that was used allowed the cyclic voltammograms to be recorded under oxygen- and moisture-free conditions. A platinum disk (area = 0.0079 cm^2) was employed as the working and auxiliary electrode. The reference electrode utilized a silver wire as a quasi-reference electrode, with the reported potential data standardized against the formal potential of the Cp_2Fe/Cp_2Fe^+ (internally added) redox couple, taken to have $E_{1/2} = 0.307$ V [15].

2.6. Extended Hückel MO calculations

The extended Hückel calculations on tbpcd and *fac*-$BrRe(CO)_3$(tbpcd) were carried out using the original program developed by Hoffmann [16], as modified by Mealli and Proserpio [17]. The weighted H_{ij}'s contained in the program were used in the calculations. The input *Z*-matrices for the model compounds tbpcd-H_4 and *fac*-$BrRe(CO)_3$(tbpcd-H_4) were constructed from the X-ray data of **1** and **2** · acetone, employing hydrogens in the place of the four ancillary phenyl groups and setting the P–H bond distances to 1.41 Å [18].

3. Results and discussion

3.1. Synthesis, spectroscopic data, and X-ray diffraction structure of tbpcd (1)

Knoevenagel condensation of the diphosphine ligand bpcd with thiophene-2-carboxaldehyde (excess) proceeds readily in CH_2Cl_2 at room temperature in the presence of added molecular sieves to afford the new diphosphine ligand 2-(2-thienylidene)-4,5-bis(diphenylphosphino)-4-cyclopenten-1,3-dione (tbpcd) in near quantitative yield. Simply stirring the two reagents without added molecular sieves showed no evidence for the formation of tbpcd (**1**), as assessed by TLC and IR analyses, which clearly underscores the need to drive the reaction to completion through the removal of the water that accompanies the Knoevenagel reaction. Compound **1** was subsequently isolated as a relatively air-stable orange solid after chromatographic separation over silica using CH_2Cl_2/petroleum ether (3:2) as the eluent. Eq. (1) illustrates the reaction leading to the tbpcd ligand.

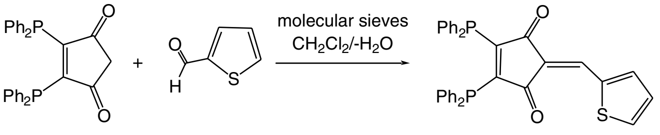

tbpcd (**1**)

(1)

The tbpcd ligand was fully characterized in solution by IR and NMR spectroscopies, ESI mass spectrometry, and X-ray diffraction analysis. The ^1H NMR spectrum of **1** confirmed the loss of the methylene hydrogens from the bpcd ligand and the formyl hydrogen from the thiophene-2-carboxaldehyde. The ^{31}P NMR spectrum displays a classic four-line AB quartet centered at δ −24.23 in keeping with the inequivalent phosphine moieties in **1**. The vibrationally coupled dione carbonyl groups of the tbpcd ligand give rise to symmetric and antisymmetric ν(CO) bands at 1719 (m) and 1673 (vs) cm^{-1} [19], that are 23 and 32 cm^{-1} lower in energy, respectively, relative to the ν(CO) bands of bpcd ligand [9,20], which in turn indicates that the tbpcd ligand is slightly more electron rich than the bpcd ligand. The UV-vis spectrum of **1** in CH_2Cl_2 is shown in Fig. 1, where a single absorbance at 374 nm ($\varepsilon = 18000$) is observed. The absorbance is insensitive to the nature of the solvent as the UV–vis band exhibits a small shift to 371 nm ($\varepsilon = 20000$) when the spectrum was recorded in MeCN solvent. The ESI mass spectrum of **1** that was recorded in the positive ion mode revealed *m*/*z* peaks at 581.086 and 558.995 for the singly charged sodium adduct of tbpcd $[\mathbf{1} + Na]^+$ and the parent ion of $[\mathbf{1}]^+$, respectively, consistent with the proposed ligand product.

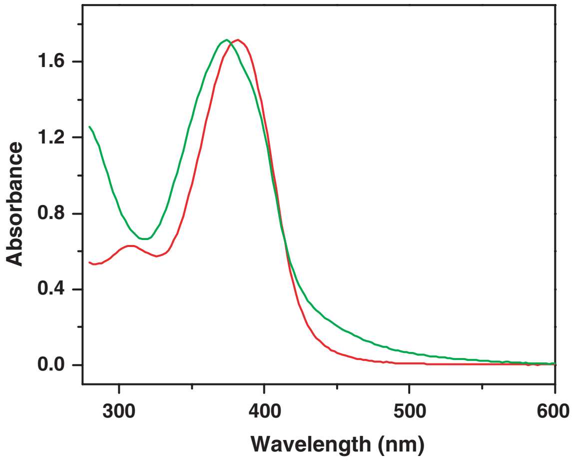

Fig. 1. UV–Vis spectra of the tbpcd ligand (green) and *fac*-BrRe-$(CO)_3$(tbpcd) (red) in CH_2Cl_2 at room temperature. Both compounds were recorded at a concentration of ca. 10^{-4} M. (For interpretation of the references to colour in this figure legend, the reader is referred to the web version of this article.)

The solid-state structure of tbpcd was determined by single-crystal X-ray diffraction analysis, with the thermal ellipsoid plot of **1** shown in Fig. 2. The union of the bpcd ligand to the formyl carbon atom of the thiophene-2-carboxaldehyde is confirmed by the presence of the exocyclic alkene moiety defined by the C(1)–C(30) vector, whose 1.352(3) Å bond length is in excellent agreement with the 1.355(3) Å bond distance found for the C(3)–C(4) π bond in the dione platform. The internuclear P(1)···P(2) bond distance of 3.330(1) Å is slightly longer than the 3.278(3) Å P···P distance reported for unsaturated diphosphine ligand (*Z*)-$Ph_2PCH{=}CHPPh_2$ [21], while the O(2)···S(2) internuclear distance of 2.861(2) Å is shorter than the sum of the van der Waals radii for oxygen and sulfur atoms by ca. 0.36 Å [22]. These structural trends indicate that the molecule is not subject to significant adverse perturbations. The two five-membered rings are essentially coplanar based on an interplanar angle of 9.1(1)°. The remaining bond distances and angles are unremarkable and require no comment.

3.2. Syntheses, spectroscopic data, and X-ray diffraction structure of *fac*-BrRe(CO)$_3$(tbpcd) (2)

The reactivity of the tbpcd ligand was next examined with the rhenium(I) compounds $BrRe(CO)_5$ and BrRe-$(CO)_3(THF)_2$ given our aforementioned interest in ligand-substituted rhenium compounds [4,6]. Our initial substitution studies employed $BrRe(CO)_5$ as a starting material. Heating an equimolar mixture of $BrRe(CO)_5$ and tbpcd at ca. 60–70 °C in either toluene or 1,2-dichloroethane furnished *fac*-$BrRe(CO)_3$(tbpcd) in good yields. TLC and IR analyses confirmed that **2** was formed as the major product. The same product was also obtained using the labile compound $BrRe(CO)_3(THF)_2$ in place of $BrRe(CO)_5$. In the case of $BrRe(CO)_3(THF)_2$, the reaction with added tbpcd ligand proceeded rapidly at room temperature to produce **2** in quantitative yield. While both rhenium starting materials give compound **2**, the use of the BrRe $(CO)_3(THF)_2$ has a slight advantage in that the reaction is cleaner and the solvent can be removed directly to give pure **2** for immediate use, if desired. The thermolysis reactions were accompanied by small amounts of unreacted

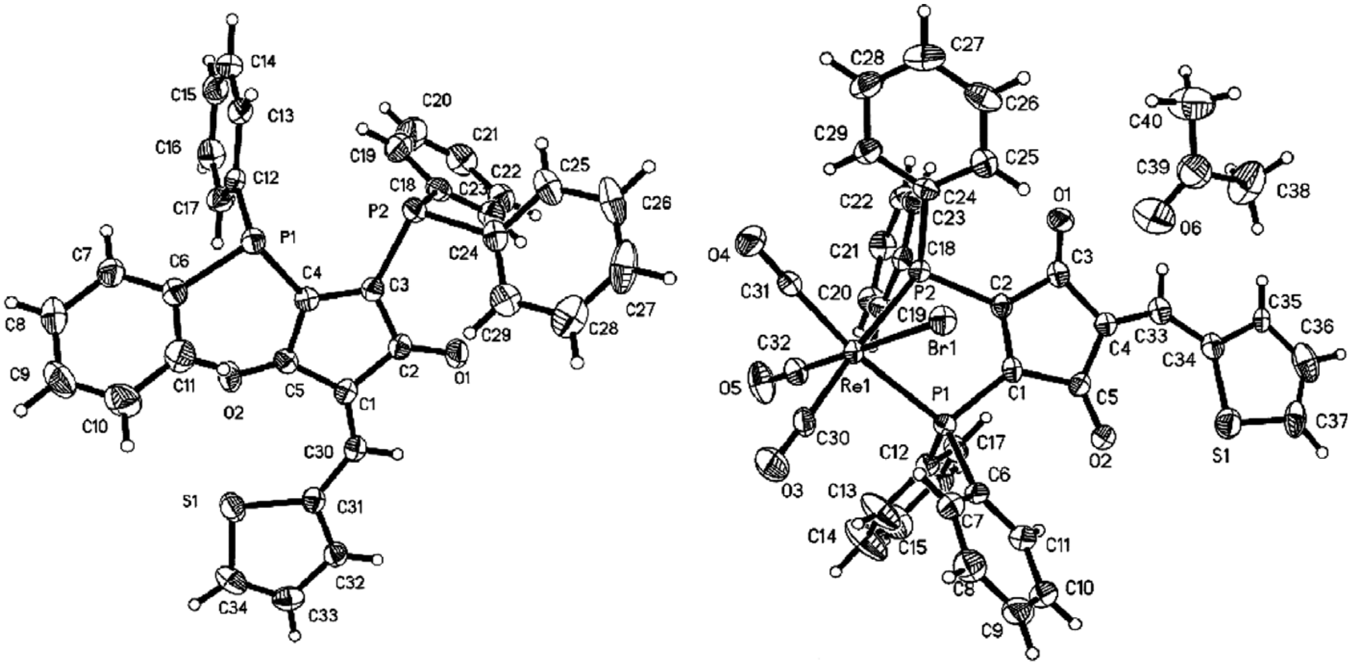

Fig. 2. Thermal ellipsoid plots of the ligand tbpcd (left) and *fac*-$BrRe(CO)_3$(tbpcd) · acetone (right) showing the thermal ellipsoids at the 50% probability level.

starting materials and unknown material(s) that remained at the origin of the TLC, necessitating a chromatographic separation. Compound **2** is air stable in the solid state, but solutions containing **2** that have been exposed to the atmosphere exhibit signs of decomposition on standing for several hours.

2 was characterized in solution by traditional spectroscopic methods, mass spectrometry (negative-ion mode), and X-ray crystallography. The IR spectrum exhibits three terminal rhenium carbonyl stretching bands at 2039 (s), 1966 (s), and 1912 (s) cm^{-1}, whose frequencies and symmetry closely match the IR data reported by us for the related compounds *fac*-BrRe$(CO)_3$(bma) and *fac*-ClRe$(CO)_3$(bpcd) [4,5]. Coordination of the tbpcd ligand to the BrRe$(CO)_3$ fragment is accompanied by a slight decrease in the electron density associated with tbpcd ligand based on the ca. 10 cm^{-1} shift of the dione ν(CO) bands to higher energy. The symmetric and antisymmetric dione carbonyl stretching bands appear at 1728 and 1684 cm^{-1}, respectively. The ^{1}H NMR data are fully consistent with the coordination of the tbpcd ligand to the *fac*-BrRe$(CO)_3$ fragment, as is the ^{31}P NMR spectrum, where two down-field singlets at δ 18.09 and 19.18 support the existence of a chelating tbpcd ligand that binds the rhenium atom via the two phosphorus moieties [23]. The UV–Vis spectrum of **2** shown in Fig. 1 exhibits a strong absorbance at 383 nm ($\varepsilon =$ 28000) and a weaker band at 308 ($\varepsilon = 9500$). The UV–vis spectrum recorded in MeCN afforded the same two-band pattern [378 nm ($\varepsilon = 35000$), 308 ($\varepsilon = 13000$)] for **2** as found in CH_2Cl_2. The ESI mass spectrum of **2** run in MeOH solvent revealed *m*/*z* peaks at 907.821 and 938.922 for the parent compound $[\mathbf{2}]^-$ and its methoxide adduct $[\mathbf{2} + \mathrm{MeO}]^-$, respectively, in agreement with the formulated structure for **2**.

The adopted coordination mode of the tbpcd ligand in **2** was established by X-ray diffraction analysis. Single crystals of **2**, as the acetone solvate, were found to exist as discrete molecules in the unit cell. The thermal ellipsoid plot of **2** is shown in the right-hand side of Fig. 1, where the chelation of the tbpcd ligand to the rhenium center by the two phosphine moieties is confirmed. The rhenium atom is six-coordinate and possesses a distorted octahedral geometry. The Re(1)–P(1) and Re(1)–P(2) distances of 2.468(1) and 2.449(1) Å, respectively, and the observed bond angle of 81.59(3)° for the P(2)–Re(1)–P(1) linkage exhibit acceptable values in comparison to those bond distances and angles in related rhenium compounds structurally characterized by us [24]. The P(1)···P(2) [3.213(2) Å] and S(1)···O(2) [2.912(3) Å] bond distances and the interplanar angle of 5.8(2)° are in agreement with those values of the free tbpcd ligand and confirm that the ancillary ligand does not experience any major structural perturbations upon coordination to the rhenium center. The remaining bond distances and angles are unexceptional and require no comment.

3.3. Cyclic voltammetry, MO calculations, and emission spectroscopy data

The cyclic voltammetric properties of the tbpcd ligand and compound **2** were next probed at a platinum disk electrode in CH_2Cl_2 solvent containing 0.2 M TBAP as the supporting electrolyte. Initially scanning a tbpcd sample at room temperature at a rate of 0.5 V/s over the potential range of 1.2 to −1.8 V revealed the presence of two reduction processes attributed to the $0/1^-$ and $1^-/2^-$ redox couples. The latter reduction exhibits a forward wave at $E_p{}^c = -1.45$ with no accompanying reverse wave ($E_p{}^a$), leading to an irreversible reduction under these conditions. Narrowing the potential window to 0 to −1.3 V and scanning just over the first reduction wave confirmed that $0/1^-$ redox couple, which displays an $E_{1/2} = -1.09$ V, is fully reversible when analyzed by standard electrochemical criteria [15]. The electron stoichiometry for the first reduction process (1e−) was also verified by comparison of the current function of the known one-electron standard ferrocene with that from tbpcd ligand. The recorded $E_{1/2}$ value for the tbpcd ligand closely matches that cyclic voltammetically determined $E_{1/2}$ value for the diphosphine ligand bpcd by Tyler and co-worker and the anthracene-functionalized bpcd ligand ($E_{1/2} = -1.01$ V) prepared by us and depicted in Scheme 1 [7,20,25].

The CV of compound **2** was recorded under identical conditions to those employed for **1**. Here the two reversible one-electron waves found at $E_{1/2} = -0.68$ and −1.39 V are readily assignable to the $0/1^-$ and $1^-/2^-$ redox couples, respectively, and parallel those data reported earlier by us for the related diphosphine complex *fac*-BrRe$(CO)_3$(bma) and the compound *fac*-BrRe$(CO)_3$(bpcd) [4,26]. It is interesting to note that the coordination of the tbpcd ligand to the rhenium center in **2** leads to enhanced stability of the $1^-/2^-$ redox couple.

That the CV data from **1** and **2** are similar and in concert with the UV–vis data for both compounds suggest that the free ligand and its rhenium complex possess common HOMO and LUMO levels. This premise was established by carrying out extended Hückel MO calculations on compounds **1** and **2**. Here the model compound 2-(2-thienylidene)-4,5-bis(diphenylphosphino-H_4)-4-cyclopenten-1,3-dione (tbpcd-H_4) was employed in our calculations, where the four ancillary phenyl groups were replaced with hydrogen atoms. The HOMO for tbpcd-H_4 occurs at −12.00 eV and is confined to the π system of the dione and thiophene rings, as shown below. The dominant contributions from the C=C π bond of the dione moiety and the carbon framework of the thiophene ring, the latter which displays a strong resemblance to ψ_2 of cyclopentadiene and other four-π-electron systems, are evident. The LUMO occurs at −10.45 eV and is strongly π^* in character and exclusively localized on the four carbon and two oxygen atoms associated with the dione platform. The nodal pattern of the LUMO is consistent with theoretical expectations for a six-π-electron system and the MO results from maleic anhydride [7,27].

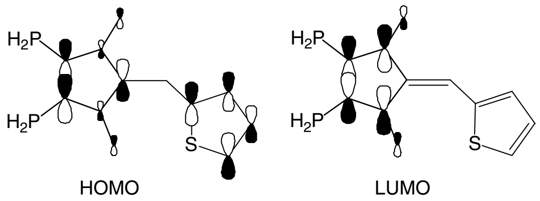

The HOMO and LUMO levels in *fac*-BrRe(CO)$_3$(tbpcd-H$_4$) were next determined so that a direct MO comparison with the free tbpcd-H$_4$ ligand could made. The calculated energies and orbital composition of the important HOMO and LUMO levels in *fac*-BrRe(CO)$_3$(tbpcd-H$_4$) were unchanged relative to the free ligand tbpcd-H$_4$. The presence of a low-lying π* LUMO that is localized on the dione moiety in *fac*-BrRe(CO)$_3$(tbpcd-H$_4$) is expected and has been theoretical and experimentally confirmed in all compounds containing an ancillary bpcd ligand investigated to date [20,28]. The surprising feature here was the composition of the HOMO level in **2** since our earlier report on *fac*-BrRe(CO)$_3$(bma) revealed that the HOMO was associated with an out-of-phase interaction involving the rhenium d_{yz} and bromine p_y orbitals with no contribution from the bma π system. Accordingly, we ran comparative Hückel calculations on *fac*-BrRe(CO)$_3$(bpcd-H$_4$) and confirmed that the LUMO (−10.44 eV) was identical to that calculated for *fac*-BrRe(CO)$_3$(bma-H$_4$) and *fac*BrRe(CO)$_3$(tbpcd-H$_4$). The HOMO in the unfunctionalized diphosphine compound *fac*-BrRe(CO)$_3$(bpcd-H$_4$) occurs at −12.35 eV and exhibits the same antibonding rhenium d_{yz} and bromine p_y interaction as found in *fac*-BrRe(CO)$_3$(bma-H$_4$) [26]. The dichotomy in the HOMO composition between *fac*-BrRe(CO)$_3$(tbpcd-H$_4$) and the corresponding bma and bpcd derivatives is readily traced to π interactions between the dione and thiophene rings in the tbpcd ligand. The extended π conjugation in the functionalized or second-generation tbpcd ligand leads to a high-lying π orbital that has no counterpart in the simple bpcd ligand. Examination of the subjacent highest-occupied molecular orbital (sHOMO) at −12.35 eV in *fac*-BrRe(CO)$_3$(tbpcd-H$_4$), which is depicted below, reveals the presence of the expected metal-based rhenium d_{yz} and bromine p_y antibonding orbital in excellent agreement with the MO data from *fac*-BrRe(CO)$_3$(bma-H$_4$) [4] and *fac*-BrRe(CO)$_3$(bpcd-H$_4$) [26].

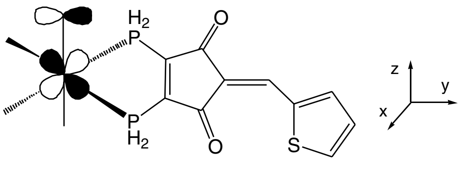

sHOMO in *fac*-BrRe(CO)$_3$(tbpcd-H$_4$)

Finally, the photophysics for compounds **1** and **2** were explored through the use of emission spectroscopy as this would allow us to corroborate experimentally the π → π* HOMO/LUMO transition indicated by the extended Hückel calculations. The emissive properties of compounds **1** and **2** were examined at room temperature in both CH_2Cl_2 and MeCN with excitation into the long wavelength band at ca. 380 nm. However, any emission displayed from either compound was not resolvable from the baseline, indicating very weak emission at best and fully consistent with the proposed intraligand π → π* transition in the free ligand and its rhenium(I) compound [29].

4. Conclusions

The synthesis of the new unsaturated diphosphine ligand 2-(2-thienylidene)-4,5-bis(diphenylphosphino)-4-cyclopenten-1,3-dione (tbpcd) from 4,5-bis(diphenylphosphino)-4-cyclopenten-1,3-dione (bpcd) and thiophene- 2-carboxaldehyde is described. The ligand substitution chemistry of the tbpcd ligand with the rhenium compounds BrRe(CO)$_5$ and BrRe(CO)$_3$(THF)$_2$ has been examined and found to furnish *fac*-BrRe(CO)$_3$(tbpcd) as the sole observable reaction product. Both new compounds have been fully characterized and their physical properties studied by a combination of methods including cyclic voltammetry, emission spectroscopy, and MO calculations.

5. Supplementary material

CCDC 623341 and 623342 contain the supplementary crystallographic data for tbpcd and *fac*-BrRe(CO)$_3$(tbpcd). These data can be obtained free of charge via http://www.ccdc.cam.ac.uk/conts/retrieving.html, or from the Cambridge Crystallographic Data Centre, 12 Union Road, Cambridge CB2 1EZ, UK; fax: (+44) 1223-336-033; or e-mail: deposit@ccdc.cam.ac.uk.

Acknowledgements

Financial support from the Robert A. Welch Foundation (Grants P-0074-WHW and B-1093-MGR) is appreciated. Prof. Andreas H. Franz (University of the Pacific) is thanked for recording the ESI-ACPI mass spectral data for the tbpcd ligand and *fac*-BrRe(CO)$_3$(tbpcd).

References

[1] (a) J.C. Luong, L. Nadjo, M.S. Wrighton, J. Am. Chem. Soc. 100 (1978) 5790;
(b) V.W.W. Yam, V.C.Y. Lau, K.K. Cheung, Orgonometallics 14 (1995) 2749;
(c) A. Vogler, H. Kunkely, Coord. Chem. Rev. 200–202 (2000) 991;
(d) D.R. Striplin, G.A. Crosby, Coord. Chem. Rev. 211 (2001) 163;
(e) J.M. Villegas, S.R. Stoyanov, W. Huang, D.R. Rillema, Inorg. Chem. 44 (2005) 2297;
(f) H. Tsubaki, A. Sekine, Y. Ohashi, K. Koike, H. Takeda, O. Ishitani, J. Am. Chem. Soc. 127 (2005) 15544.

[2] (a) P. Belser, S. Bernhard, C. Blum, A. Beyeler, L. De Cola, V. Balzani, Coord. Chem. Rev. 190–192 (1999) 190;
(b) A. Beyeler, P. Belser, L. De Cola, Angew. Chem., Int. Ed. Engl. 36 (1997) 2779;
(c) W. Belliston-Bittner, R. Alexander, Y.H.L. Nguyen, D.J. Stuehr, J.R. Winkler, H.B. Gray, J. Am. Chem. Soc. 127 (2005) 15907.

[3] (a) S.Y. Reece, D.G. Nocera, J. Am. Chem. Soc. 127 (2005) 9448;
(b) S.Y. Reece, M.R. Seyedsayamdost, J. Stubbe, D.G. Nocera, J. Am. Chem. Soc. 128 (2006) 13654.

[4] K. Yang, S.G. Bott, M.G. Richmond, Organometallics 14 (1995) 2387.

[5] W.H. Watson, S. Kandala, M.G. Richmond, J. Chem. Crystallogr. 36 (2006) 77.

[6] G. Wu, D.R. Glass, D. May, W.H. Watson, D. Wiedenfeld, M.G. Richmond, J. Organomet. Chem. 690 (2005) 4993.

[7] W.H. Watson, B. Poola, M.G. Richmond, J. Chem. Crystallogr. 36 (2006) 715.

[8] For an earlier report describing Knoevenagel-type condensation reactions with 4,5-dichloro- 4-cyclopenten-1,3-dione, the starting material for the ligand bpcd, see: R. Alfred, Z. Hellmut, Chem. Ber. 94 (1961) 1800.

[9] (a) D. Fenske, H. Becher, Chem. Ber. 107 (1974) 117;
(b) D. Fenske, Chem. Ber. 112 (1979) 363.

[10] (a) D. Vitali, F. Calderazzo, Gazz. Chim. Ital. 102 (1972) 587;
(b) F. Calderazzo, I.P. Mavani, D. Vatali, I. Bernal, J.D. Korp, J.L. Atwood, J. Organomet. Chem. 160 (1978) 207.

[11] D.F. Shriver, The Manipulation of Air-Sensitive Compounds, McGraw-Hill, New York, 1969.

[12] SAINT Version 6.02, Bruker Analytical X-ray Systems Inc., Copyright 1997–1999.

[13] SHELXTL Version 5.1, Bruker Analytical X-ray Systems Inc., Copyright 1998.

[14] A.L. Spek, PLATON – A Multipurpose Crystallographic Tool, Utrecht University, Utrecht, The Netherlands, 2001.

[15] A.J. Bard, L.R. Faulkner, Electrochemical Methods, Wiley, New York, 1980.

[16] (a) R. Hoffmann, W.H. Lipscomb, J. Chem. Phys. 36 (1962) 2179;
(b) R. Hoffmann, J. Chem. Phys. 39 (1963) 1397.

[17] C. Mealli, D.M. Proserpio, J. Chem. Ed. 67 (1990) 399.

[18] R.C. Weast (Ed.), Handbook of Chemistry and Physics, 56th ed., CRC Press, Cleveland, OH, 1975.

[19] N.B. Coltrup, L.H. Daly, S.E. Wiberley, Introduction to Infrared and Raman Spectroscopy, Academic Press, New York, 1990.

[20] R. Meyer, D.M. Schut, K.J. Keana, D.R. Tyler, Inorg. Chim. Acta 240 (1995) 405.

[21] S.J. Berners, L.A. Colquhoun, P.C. Healy, K.A. Byriel, J.V. Hanna, J. Chem. Soc., Dalton Trans. (1992) 3357.

[22] A. Bondi, J. Phys. Chem. 68 (1968) 441.

[23] P.E. Garrou, Chem. Rev. 81 (1981) 229.

[24] (a) S.G. Bott, K. Yang, M.G. Richmond, J. Organomet. Chem. 689 (2004) 791;
(b) S.G. Bott, K. Yang, M.G. Richmond, J. Chem. Crystallogr. 35 (2005) 709;
(c) C.-G. Xia, S.G. Bott, M.G. Richmond, Inorg. Chim. Acta 230 (1995) 45.

[25] For an earlier electrochemical investigation of the bpcd ligand using polarographic methods, see: H.J. Becher, D. Fenske, M. Heyman, Z. Anorg. Allg. Chem. 475 (1981) 27.

[26] Unpublished results.

[27] (a) T.A. Albright, J.K. Burdett, M.H. Whangbo, Orbital Interactions in Chemistry, Wiley-Interscience, New York, 1985;
(b) K. Hayakawa, N. Mibu, E. Osawa, K. Kanematsu, J. Am. Chem. Soc. 104 (1982) 7136.

[28] (a) H. Shen, S.G. Bott, M.G. Richmond, Organometallics 14 (1995) 4625;
(b) N.W. Duffy, R.R. Nelson, M.G. Richmond, A.L. Rieger, P.H. Rieger, B.H. Robinson, D.R. Tyler, J.C. Wang, K. Yang, Inorg. Chem. 37 (1998) 4849;
(c) S.G. Bott, H. Shen, M.G. Richmond, J. Organomet. Chem. 689 (2004) 3426.

[29] G.L. Geoffroy, M.S. Wrighton, Organometallic Photochemistry, Academic Press, New York, 1979.